*Laser and Particle Beams* (2012), *30*, 671–677.

doi:10.1017/S0263034612000559

# Two-dimensional quantum hydrodynamic model for the heating of a solid target using a Gaussian cluster

YA ZHANG,[1] YUAN-HONG SONG,[1] YONG-TAO ZHAO,[2] AND YOU-NIAN WANG[1]

[1]School of Physics and Optoelectronic Technology, Dalian University of Technology, Dalian, China
[2]Institute of Modern Physics, Chinese Academy of Sciences, Lanzhou China

(RECEIVED 23 April 2012; ACCEPTED 12 July 2012)

**Abstract**

This paper presents numerical simulations to study the heating of a two-dimensional (2D) solid target under an ion cluster interaction. 2D quantum hydrodynamic (QHD) model is employed for the heating of solid target to warm dense matter on a picosecond time scale. A Gaussian cluster is used to uniformly heat the solid target to a temperature of several eV. The density and temperature of the target are calculated by a full self-consistent treatment of the QHD formalisms and the Poisson's equation. The technique described in this paper provides a method for creating uniformly heated strongly coupled plasma states.

**Keywords:** Cluster; Uniform heating; Warm dense matter

## 1. INTRODUCTION

Interaction processes of ion beam or cluster with matter are important for the applications in basic and applied physics (Patel *et al.,* 2003; Brambrink *et al.,* 2006; Tahir *et al.,* 2009*a*), laboratory accelerator (Tahir *et al.,* 2009*b*), inertial confinement fusion (ICF) (Deutsch, 1986; Deutsch *et al.,* 1989; Hora, 2007; Hoffmann, 2008), astrophysical processes (Nettelmann *et al.*, 2008), heavy ion beam research (Hoffmann *et al.*, 2010; Stöckl *et al.,* 1996; Tahir *et al.,* 2007*)*, and high energy density physics (HEDP) (Tahir *et al.,* 2005; Nellis, 2006; Hoffmann *et al.,* 2009). HEDP is understood to be the thermodynamic regime where the energy density exceeds $10^{11}$ J/m$^3$ or equivalent pressure of 1 Mbar and above. Pioneering experiments of beam-matter interactions (Deutsch *et al.,* 1989) have been conducted to investigate the stopping power for hydrogen plasma, which have demonstrated that the stopping power can increase with the increasing ionization of plasma due to the free electrons interacting with beam ions. It will be shown very soon that intense clusters may be of considerable potential interest for driving an ICF (Deutsch, 1992). Using clusters as a ICF driver, can break through the space-charge limit of ion beam, which is helpful to achieve high heating effect. Recently, several attempts have been made to investigate the beam-matter interactions involving heavy ion (Zhao *et al.*, 2009; Hoffmann *et al.*, 2010), proton (Patel *et al.,* 2003; Tahir *et al.*, 2009a) and laser beams (Zhao *et al.,* 2012). In particular, ICF is a promising scheme, where a target matter can be irradiated by intense ion beams or clusters, and be transformed into a plasma of high density and high temperature which can initiate fusion reactions (Deutsch, 1992; Tahir *et al.,* 2005).

The basic properties of interactions between ions and matter, which play an essential role in the above scenario, have been encouraged to be explored thoroughly. The evaluations of target temperature and density are an ideal tool to investigate these interactions for ion beams or clusters immersed in a target. It is expected in such studies that target properties would be influenced significantly by the modulation of beam or cluster parameters such as particle energy, total number of particles per beam, and focal spot size. These beam parameters will be available at the new powerful heavy ion synchrotron, SIS100, at GSI Darmstadt, which will deliver strongly bunched intense beams and clusters of all stable ion species from protons up to uranium with particle energies a few MeV-GeV/u (Tahir *et al.*, 2009*a*, 2011*)*. These intense ion beams and clusters present a promising source for volumetric heating and bring up unique capabilities for HEDP. In this field, one of the special interests is warm dense matter (WDM) research, since the accelerator technology has improved sufficiently to provide intense ion beams and clusters to heat samples of target and reach the

Address correspondence and reprint requests to: You-Nian Wang, School of Physics and Optoelectronic Technology, Dalian University of Technology, Dalian 116024, China. E-mail: ynwang@dlut.edu.cn.

regime of WDM. WDM is the region in temperature (several eV) and density that can be described as strongly coupled plasma. The importance of WDM arises from its wide occurrence, namely planetary science, cold star physics, and all plasma production devices, which start from cold dense matter.

In a strong coupling plasma considering nonlinear effects, the interaction processes of ions with matter have been simulated by employing various methods, such as particle-in-cell (PIC) and molecular-dynamics (MD) (Zwicknagel *et al.,* 1999; Hu *et al.*, 2011, 2012). In particular, quantum hydrodynamic (QHD) model has been developed by solving the nonlinear Schördinger-Poisson or the Wigner-Poisson kinetic models, which can be devoted to studying the properties of strongly coupled plasmas. Large number of calculations have been carried out by using the QHD model since the use of this theory was introduced (Chen *et al.,* 1995; Haas *et al.,* 2000; Manfredi and Haas, 2001*)*, due to the advantages that the QHD equations are quite simple for numerical studies and have a straightforward interpretation in terms of fluid quantities that are employed in classical physics. In our previous work (Zhang *et al.,* 2011*b*), we have simulated the wake potential and energy loss of a test charge propagating in a one-dimensional (1D) solid target, by using the 1D QHD theory. However, the QHD theory has not been applied to examine an ion cluster interacting with a two-dimensional (2D) solid target so far.

The aim of this paper is to extend our previous work (Zhang *et al.*, 2011*b)* to a 2D case with an ion cluster interaction, moreover, the energy-balance equation is considered in this work. The 2D QHD approach will be employed to analyze the isochoric heating (i.e., heating at constant volume) of aluminum solid target under an ion cluster interaction, which can heat solid density material to warm dense states on a picosecond time scale. We shall show how the temperature and density of the target are affected by the modulation of cluster properties and how the WDM is generated from a cold target. The nonlinear QHD equations will be solved by employing the flux-corrected-transport (FCT) method (Boris *et al.*, 1993), which has proven to be an accurate and easy to use algorithm to solve nonlinear time-dependent conservative equations of hydrodynamics. This paper is organized as follows. In Section 2, the nonlinear 2D QHD formalisms coupled with the Poisson's equation, are presented. In Section 3, we show numerical results of the temperature and density of the target. Finally, a short summary is given in Section 4. Gauss units will be adopted throughout the paper except specific definition.

## 2. QUANTUM HYDRODYNAMIC MODEL

We consider a Gaussian proton cluster of density profile $n_c\ (z,\ r,\ t) = n_{c0}\ exp(-r^2/r_c^2 - (z - V_c t)^2/l_c^2)$ with cluster radius $r_c$ and cluster half-length $l_c$, propagating with constant velocity $V_c = \sqrt{2E_{cp}/m_{cp}}$ through a solid aluminum target along the $z$ axis. Here, $m_{cp}$ is the proton mass and $E_{cp}$ is the proton energy. The total number of protons $N_{cp}$ within cluster is $N_{cp} = 4\pi \int_0^{l_c} \int_0^{r_c} n_c\ (z, r, t)\ rdrdz$, functions of $n_{c0}$, $r_c$, and $l_c$. Note that the total number and Gaussian distribution of protons within cluster are unvaried with time $t$ evaluation. We treat the valence electrons in the target as free electrons with an equilibrium density $n_0 = 7.829 \times 10^{+23}\ \mathrm{cm}^{-3}$, which is aluminum solid density, immersed in a uniform background of motionless ions. The electron dynamics can be analyzed by a collective-stimulated interaction model, that is, the transmission of the cluster ions can cause dynamics polarization effect in the target.

The simulation technique is the 2D QHD model with the electron velocity field $\mathbf{u}_e\ (z,\ r,\ t)$, density $n_e\ (z,\ r,\ t)$, and energy density $W_e\ (z,\ r,\ t)$ by the continuity equation

$$\frac{\partial n_e}{\partial t} + \nabla \cdot (n_e \mathbf{u}_e) = 0, \tag{1}$$

the momentum-balance equation

$$\begin{aligned} \frac{\partial \mathbf{u}_e}{\partial t} + (\mathbf{u}_e \cdot \nabla)\mathbf{u}_e = \frac{e}{m_e}\nabla\Phi - \frac{\nabla P_e}{m_e n_e} \\ + \frac{\hbar^2}{2m_e^2}\nabla\left(\frac{1}{\sqrt{n_e}}\nabla^2\sqrt{n_e}\right) - \gamma \mathbf{u}_e, \end{aligned} \tag{2}$$

and the energy-balance equation (Chen *et al.,* 1995)

$$\begin{aligned} \frac{\partial W_e}{\partial t} + \nabla \cdot (W_e \mathbf{u}_e) = e n_e \mathbf{u}_e \cdot \nabla\Phi - \nabla \cdot (\mathbf{u}_e P_e) \\ - \nabla \cdot \mathbf{q}_e - \frac{W_e - \frac{3}{2} n_e T_e}{\tau_w}, \end{aligned} \tag{3}$$

with $W_e = \frac{3}{2} n_e T_e + \frac{1}{2} m_e n_e u_e^2 - \frac{\hbar^2 n_e}{24 m_e}\nabla^2 \log(n_e) + O(\hbar^4)$. The above equations are closed by adding Poisson's equation

$$\nabla^2\Phi = 4\pi e(n_e - n_0 - Z_1 n_c). \tag{4}$$

Here, $\nabla = \frac{\partial}{\partial r}\mathbf{e}_r + \frac{\partial}{\partial z}\mathbf{e}_z$, $m_e$ is the electron mass, $e$ is the elementary charge, $\Phi$ is the total electric potential, $\mathbf{q}_e$, $T_e$, and $P_e$ are the electron heat flux, temperature and pressure, respectively, $\gamma$ and $\tau_w$ are the frictional coefficients with $\tau_w = 2\gamma$. In particular, the electron pressure $P_e$ can be calculated by finite temperature Thomas-Fermi theory (More *et al.,* 1988) and the heat flux is specified by Fourier's law $\mathbf{q}_e = -\kappa\ \nabla\ T_e$ (Chen *et al.,* 1995) with thermal conductivity $\kappa$. In the right-hand side, the second and third terms of Eq. (2) are regarded as the quantum effects, and the last terms of Eqs. (2) and (3) are the frictional forces with $\gamma$ and $\tau_w$ obtained from our previous work *(Zhang et al.*, 2011*a)*.

The above Eqs. (1)–(4) involve a self-consistent determination of the electron density, velocity, and temperature, and the total electric field $\mathbf{E} = -\nabla\Phi$ with the components $E_r$ and $E_z$. The FCT method is adopted to numerically solve Eqs. (1)–(3) by split-time integration from the initial time $t = 0$ when the values of all quantities are known. The

https://doi.org/10.1017/S0263034612000559 Published online by Cambridge University Press

Poisson's equation is solved by the successive over relaxation (SOR) method.

In the following section, we obtain the numerical values of the density and temperature of the target under the effect of a Gaussian proton cluster. In the simulation, $n_{c0} = n_0 \times 10^{-9}$ and the cluster is projected from ($z = 0$, $r = 0$) at $t = 0$. Our numerical results are obtained for solid aluminum with initial solid density $n_0$ and initial temperature $T_e = 0$ eV.

## 3. NUMERICAL RESULTS

Figure 1 show the density as functions of $r$ and $z$ at 5 ps Figure 1a and 10 ps Figure 1b for $E_{cp} = 20$ MeV, and at 5 ps Figure 1c and 10 ps Figure 1d for $E_{cp} = 10$ MeV. Here, $r_c = 3$ μm and $l_c = 15$ μm. The density demonstrates a clear time and space variations and wake effects are generated behind the cluster. A comparison between Figuers 1a and 1b shows that the maximum density is almost unchanged with the cluster penetration time. As the cluster penetrates deeper into the target, the perturbed density region becomes larger. When $E_{cp} = 20$ MeV in Figures 1a–b, the range of the cluster is longer, while the maximum density is smaller, in comparison with that for $E_{cp} = 10$ MeV in Figures 1c–1d. The perturbed density decreases and tends to reach an initial equilibrium value with the increasing distance behind the cluster.

Temperature corresponding to Figures 1a–1d is shown in Figures 2a–2d. Cluster protons impinging on the target deposit their energy in the target that leads to an increase in the temperature. Thus the spatial profile of the temperature is similar to the Gaussian distribution of the cluster. In the cluster heated region, temperature of $0.6 \leq T_e \leq 1$ eV is obtained in Figures 2a–2b and that of $1 \leq T_e \leq 1.5$ eV is obtained in Figures 2c–2d, where WDM is generated. The WDM temperature range is roughly $T_e = 1.0$–$20$ eV for aluminum. As the cluster transmission time increases, a larger volume of the target has been heated. When $E_{cp} =$ 20 MeV in Figures 2a–2b, the range of the cluster is longer and the heated region is larger, while the maximum temperature is smaller, in comparison with those for $E_{cp} = 10$ MeV in Figures 2c–2d. Moreover, more uniform temperature is obtained in Figs. 2(a-b), as compared to that shown in Figures 2c–2d. Note that nearly uniform temperature of several eV is achieved in the cluster heated region and the target can be converted into WDM on a picosecond time scale, which is important for the study of HEDP and ICF research.

To further examine the influence of the cluster parameters on the density, we present in Figures 3a–3c the density as functions of $r$ and $z$ with $r_c = 1$ μm, $l_c = 10$ μm Figure 3a, $r_c = 3$ μm, $l_c = 15$ μm Figure 3b and $r_c = 6$ μm, $l_c = 20$ μm Figure 3c. Here, $E_{cp} = 20$ MeV and $t = 10$ ps. In Figures 3a–3b the maximum density decreases with decreasing $r_c$ and $l_c$ due to reduction in $n_c$ that has a direct ratio relation with $r_c$ and $l_c$.

Temperature corresponding to Figures 3a–3c, is presented in Figures 4a–4c. It is clearly seen in Figures 4a–4c where the cluster heated volume becomes larger in radial direction and the maximum temperature increases with increasing $r_c$ and $l_c$. The temperature exhibits a nearly uniform distribution in the cluster heated region, which has values of $T_e = 0.4 \sim 2$ eV. Moreover, the maximum temperature (2 eV) is in favor of important experiments on HEDP.

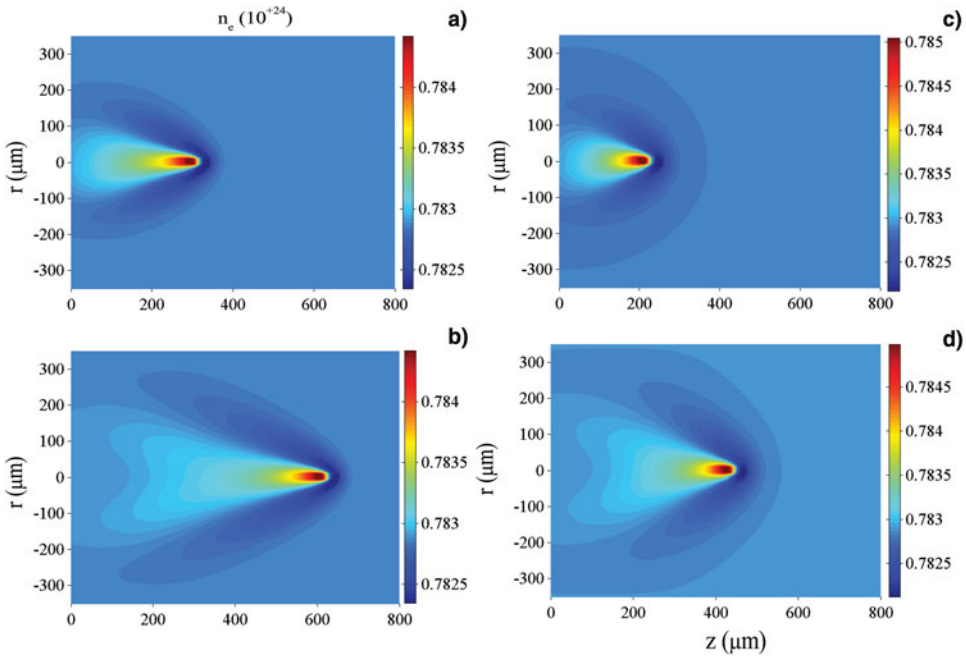


**Fig. 1.** (Color online) The density at 5 ps (**a**) and 10 ps (**b**) for $E_{cp} = 20$ MeV, and at 5 ps (**c**) and 10 ps (**d**) for $E_{cp} = 10$ MeV. Here, $r_c = 3$ μm and $l_c = 15$ μm.

https://doi.org/10.1017/S0263034612000559 Published online by Cambridge University Press

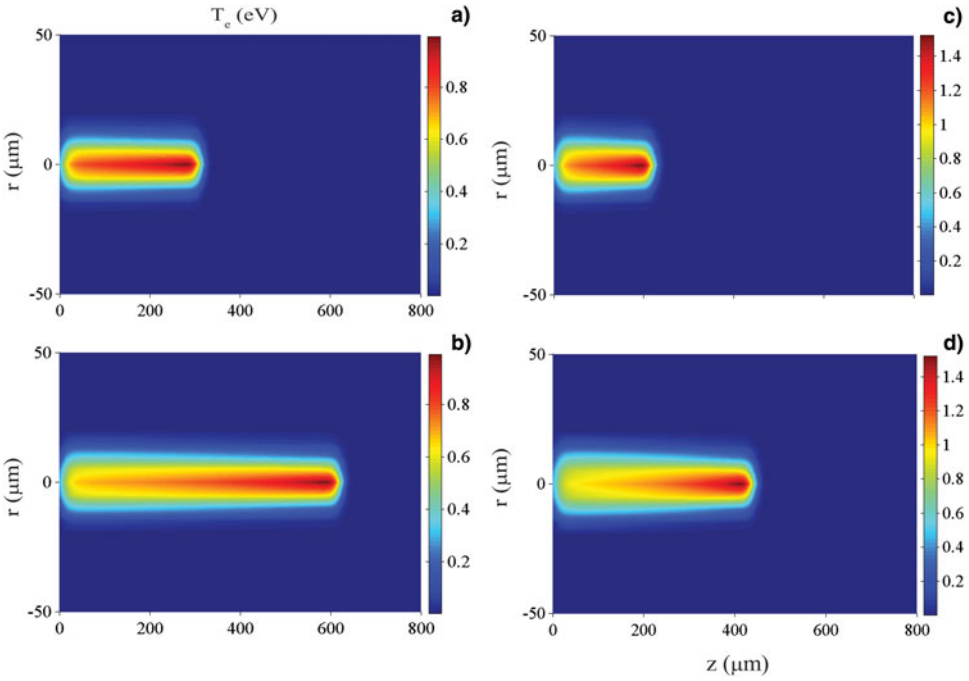


**Fig. 2.** (Color online) The temperature at 5 ps (**a**) and 10 ps (**b**) for $E_{cp} = 20$ MeV, and at 5 ps (**c**) and 10 ps (**d**) for $E_{cp} = 10$ MeV. Here, $r_c = 3$ μm and $l_c = 15$ μm.

The density and temperature are significantly impacted by the cluster properties, as a result, such a influence is also shown in the total electric field. Corresponding to Figure 3b and Figure 3c, Figures 5a–5b and Figures 5c–5d show $E_r$ and $E_z$ as functions of $r$ and $z$, with $E_r$ Figure 5a and $E_z$ Figure 5b for $r_c = 3$ μm, $l_c = 15$ μm and $E_r$ Figure 5c and $E_z$ Figure 5d for $r_c = 6$ μm, $l_c = 20$ μm. Here, $E_{cp} = 20$ MeV and $t = 10$ ps. The total electric field is mainly determined by the Gaussian cluster, so the initial values $E_r = 0$, $E_z = 0$ are changed only at and around the cluster center, as shown in Figures 5a–5d. The volume of nonzero electric fields is smaller for a lower $r_c$ and $l_c$ due to reduction in $n_c$. The spectrum

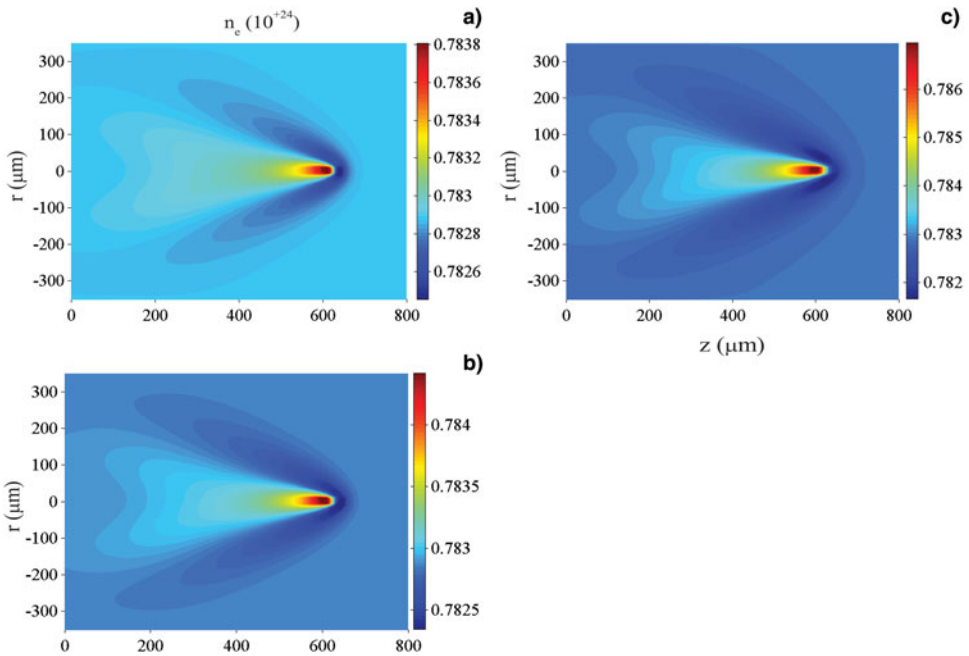


**Fig. 3.** (Color online) The density with $r_c = 1$ μm, $l_c = 10$ μm (**a**), $r_c = 3$ μm, $l_c = 15$ μm (**b**) and $r_c = 6$ μm, $l_c = 20$μm (**c**). Here, $E_{cp} = 20$ MeV and $t = 10$ ps.

https://doi.org/10.1017/S0263034612000559 Published online by Cambridge University Press

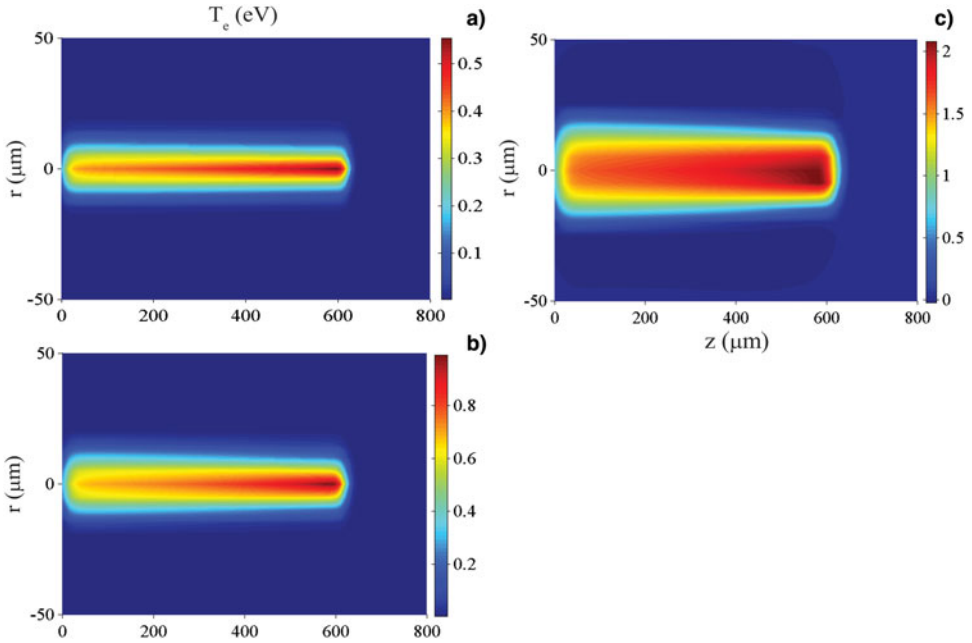


**Fig. 4.** (Color online) The temperature with $r_c = 1$ μm, $l_c = 10$ μm (**a**), $r_c = 3$ μm, $l_c = 15$ μm (**b**) and $r_c = 6$ μm, $l_c = 20$ μm (**c**). Here, $E_{cp} = 20$ MeV and $t = 10$ ps.

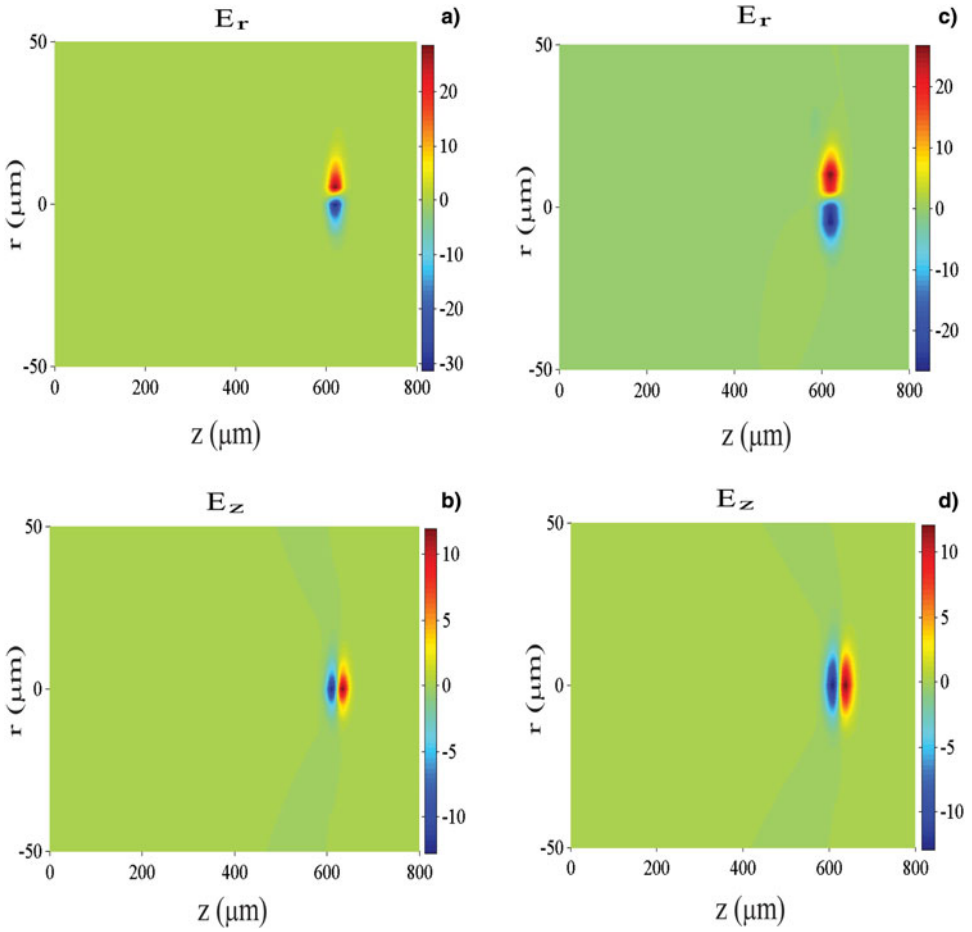


**Fig. 5.** (Color online) $E_r$ (**a**) and $E_z$ (**b**) for $r_c = 3$ μm, $l_c = 15$ μm and $E_r$ (**c**) and $E_z$ (**d**) for $r_c = 6$ μm, $l_c = 20$ μm. Here, $E_{cp} = 20$ MeV and $t = 10$ ps.

https://doi.org/10.1017/S0263034612000559 Published online by Cambridge University Press

of $E_r$ displays an antisymmetry, while $E_z$ is symmetric, with respect to the axis ($r = 0$).

## 4. CONCLUSIONS

Numerical simulations of interaction of a Gaussian proton cluster with 2D aluminum solid target are carried out. 2D QHD model is employed for the heating of solid target. A full self-consistent treatment of this problem requires coupling of the QHD formalisms with the Poisson's equation. The density and temperature of the target and the total electric field, are calculated by solving the QHD equations and the Poisson's equation. The FCT method is adopted to numerically solve the nonlinear QHD equations. The Poisson's equation is solved by the SOR method. As the cluster penetrates into the target, a uniform temperature distribution is displayed in the cluster heated region. It is interesting to note that the target is heated to a few eV and a WDM matter is generated in the cluster heated region on a picosecond time scale. Therefore, one can access the very interesting but almost unexplored strongly coupled plasma state in this work.

In the near future, this work could be modified to consider interactions of an intense ion beam pulse with solid target by using double QHD model for beam and target particles, where high energy density (HED) matter can be generated. The developments of high-quality well-focused strongly bunched intense ion beams, from a facility of antiproton and ion research (FAIR) at GSI Darmstadt, can lead to generating samples of HED matter through isochoric and uniform heating of solid targets by such intense beams.

## ACKNOWLEDGMENT

This work was supported by the National Basic Research Program of China (Grants No. 2010CB832901), Fundamental Research Funds for the Central Universities (Grant No. DUT10ZD111), National Natural Science Foundation of China (Grant No.10975028), and the Program for New Century Excellent Talents in University (NCET-08-0073).

## REFERENCES

Boris, J.P., Landsberg, A.M., Oran, E.S. & Gardner, J.H. (1993). LCPFCT–flux-corrected transport algorithm for solving generalized continuity equations. In *NRL Memorandom Report* **6410**. Washington, DC: Naval Research Laboratory, 20375–5320.

Brambrink, E., Roth, M., Blazevic, A. & Schlegel, T. (2006). Modeling of the electrostatic sheath shape on the rear target surface in short-pulse laser-driven proton acceleration. *Laser Part. Beams* **24**, 163–168.

Chen, Z., Cockburn, B., Gardner, C.L. & Jerome, J.W. (1995). Quantum hydrodynamic simulation of hysteresis in the resonant tunneling diode. *J. Comput. Phys.* **117**, 274–280.

Deutsch, C. (1986). Inertial confinement fusion driven by intense ion beams. *Ann. Phys. (Paris)* **11**, 1–111.

Deutsch, C., Maynard, G., Bimbot, R., Gardes, D., Dellanegra, S., Dumail, M., Kubica, B., Richard, A., River, M.F., Sernagean, A., Fleurier, C., Sanba, A., Hoffmann, D.H.H., Weyrich, K. & Wahl, H. (1989). Ion beam-plasma interaction: A standard model approach. *Nucl. Instrum. Methods Phys. Res. A* **278**, 38–43.

Deutsch, C. (1992). Ion cluster interaction with cold targets for ICF: Fragmentation and stopping. *Laser Part. Beams* **10**, 217–226.

Haas, F., Manfredi, G. & Feix, M. (2000). Multistream model for quantum plasmas. *Phys. Rev. E* **62**, 2763.

Hoffmann, D.H.H. (2008). Intense laser and particle beams interaction physics toward inertial fusion. *Laser Part. Beams* **26**, 295–296.

Hoffmann, D.H.H., Fortov, V.E., Kuster, M., Mintsev, V., Sharkov, B.Y., Tahir, N.A., Udrea, S., Varentsov, D. & Weyrich, K. (2009). High energy density physics generated by intense heavy ion beams. *Astrophys Space Sci.* **322**, 167–177.

Hoffmann, D.H.H., Tahir, N.A., Udreal, S., Rosmej, O., Meister, C.V., Varentsov, D., Roth, M., Schaumann, G., Frank, A., Blažević, A., Ling, J., Hug, A., Menzel, J., Hessling, TH., Harres, K., Günther, M., El-Moussatil, S., Schumacher, D. & Imran, M. (2010). High energy density physics with heavy ion beams and related interaction phenomena. *Contrib. Plasma Phys.* **50**, 7–15.

Hora, H. (2007). New aspects for fusion energy using inertial confinement. *Laser Part. Beams* **25**, 37–45.

Hu, Z.-H., Song, Y.-H., Mišković, Z.L. & Wang, Y.-N. (2011). Energy dissipation of ion beam in two-component plasma in the presence of laser irradiation. *Laser Part. Beams* **29**, 299–304.

Hu, Z.-H., Song, Y.-H. & Wang, Y.-N. (2012). Time evolution and energy deposition for ion clusters injected into magnetized two-component plasmas. *Phys. Rev. E* **85**, 016402.

Manfredi, G. & Haas, F. (2001). Self-consistent fluid model for a quantum electron gas. *Phys. Rev. B* **64**, 075316.

More, R.M., Warren, K.H., Young, D.A. & Zimmerman, G.B. (1988). A new quotidian equation of state (QEOS) for hot dense matter. *Phys. Fluids* **31**, 3059–3078.

Nellis, W.J. (2006). Dynamic compression of materials: Metallization of fluid hydrogen at high pressures. *Rep. Prog. Phys.* **69**, 1479–1580.

Nettelmann, N., Holst, B., Kietzmann, A., French, M., Redmer, R. & Blaschke, D. (2008). Ab initio equation of state data for hydrogen, helium, and water and the internal structure of Jupiter. *Astrophysic. J.* **683**, 1217–1228.

Patel, P.K., Mackinnon, A.J., Key, M.H., Cowan, T.E., Foord, M.E., Allen, M., Price, D.F. & Ruhl, H. (2003). Isochoric heating of solid-density matter with an ultrafast proton beam. *Phys. Rev. Lett.* **91**, 125004.

Stöckl, C., Frankenheim, O.B., Roth, M., Suß, W., Wetzler, H., Seelig, W., Kulish, M., Dornik, M., Laux, W., Spiller, P., Stetter, M., Stöwe, S., Jacoby, J. & Hoffmann, D.H.H. (1996). Interaction of heavy ion beams with dense plasmas. *Laser Part. Beams* **14**, 561–574.

Tahir, N.A., Deutsch, C., Fortov, V.E., Gryaznov, V., Hoffmann, D.H.H., Kulish, M., Lomonosov, I.V., Mintsev, V., Ni, P., Nikolaev, D., Piriz, A.R., Shilkin, N., Spiller, P., Shutov, A., Temporal, M., Ternovoi, V., Udrea, S. & Varentsov, D. (2005). Proposal for the study of thermophysical properties of high-energy-density matter using current and future heavy-ion accelerator facilities at GSI Darmstadt. *Phys. Rev. Lett.* **95**, 035001.

Tahir, N.A., Kim, V., Matvechev, A., Ostrik, A., Lomonosov, I.V., Piriz, A.R., Cela, J.J.L. & Hoffmann, D.H.H. (2007). Numerical modeling of heavy ion induced stress waves in solid targets. *Laser Part. Beams* **25**, 523–540.

Tahir, N.A., Schmidt, R., Shutov, A., Lomonosov, I.V., Piriz, A.R., Hoffmann, D.H.H., Deutsch, C. & Fortov, V.E. (2009*a*). Large hadron collider at CERN: Beams generating high-energy-density matter. *Phys. Rev. E* **79**, 046410.

Tahir, N.A., Spiller, P., Shutov, A., Lomonosov, I.V., Piriz, A.R., Redmer, R., Hoffmann, D.H.H., Fortov, V.E., Deutsch, C. & Bock, R.M. (2009*b*). Proposed high energy density physics research using intense particle beams at FAIR: The HEDgeHOB collaboration. *IEEE Trans. Plasma Sci.* **37**, 1267–1275.

Tahir, N.A., Shutov, A., Piriz, A.R., Lomonosov, I.V., Deutsch, C., Spiller, P. & Stöhlker, TH. (2011). Application of intense heavy ion beams to study high energy density physics. *Plasma Phys. Control. Fusion* **53**, 124004.

Zhang, Y., Song, Y.-H. & Wang, Y.-N. (2011*a*). Stopping power for a charged particle moving through three-dimensional nonideal finite-temperature electron gases. *Phys. Plasmas* **18**, 072701.

Zhang, Y., Song, Y.-H. & Wang, Y.-N. (2011*b*). Nonlinear wake potential and stopping power for charged particles interacting with a one-dimensional electron gas. *Phys. Plasmas* **18**, 112705.

Zhao, Y., Xu, H., Zhao, H., Xia, J., Jin, G., Ma, X., Liu, Y., Yang, Z., Zhang, P., Wang, Y., Li, D., Zhao, H., Zhan, W., Xu, Z., Zhao, D., Li, F. & Chen, X. (2009). An outlook of heavy ion driven plasma research at IMP-Lanzhou. *Nucl. Instrum. Meth. Phys. Res. B* **267**, 163–166.

Zhao, X. & Shin, Y.C. (2012). A two-dimensional comprehensive hydrodynamic model for femtosecond laser pulse interaction with metals. *J. Phys. D: Appl. Phys.* **45**, 105201.

Zwicknagel, G., Toepffer, C. & Reinhard, P.G. (1999). Stopping of heavy ions in plasmas at strong coupling. *Phys. Rep.* **309**, 117–208.

https://doi.org/10.1017/S0263034612000559 Published online by Cambridge University Press